International Journal of Engineering

Journal Homepage: www.ije.ir

Ranking Passive Seismic Control Systems by Their Effectiveness in Reducing Responses of High-Rise Buildings with Concrete Shear Walls Using Multiple-Criteria Decision Making

M. S. Barkhordari, M. Tehranizadeh*

Department of Civil and Environmental Engineering, Amirkabir University of Technology, Tehran, Iran

P A P E R I N F O

Paper history:
Received 09 April 2020
Received in revised form 21 April 2020
Accepted 12 June 2020

Keywords:
Concrete Shear Walls
Multiple-Criteria Decision-Making Method
Opensees
Passive Control Systems
Tall Buildings

A B S T R A C T

In recent decades, the dual systems of steel moment-resisting frames and RC shear walls have found extensive application as lateral load-resisting systems for high-rise structures in seismically active areas. This paper investigated the effectiveness of tuned mass damper (TMD), viscous damper, friction damper, and the lead-core rubber bearing in controlling the damage and seismic response of high-rise structures with concrete shear walls. Five buildings (10, 15, 20, 25, and 30-story) with passive seismic control systems were analyzed in OpenSees using 50 seismic records. The structural responses (acceleration, drift, displacement, velocity, and base shear) were adopted as the criteria. The criteria were nondimensionalized by defining a measure to establish a relationship between the inputs (ground motions) and outputs (structural responses). At the end, Multi Criterion Decision Making (MCDM) method was employed to rank the passive seismic control systems and select the best one. The results showed application of the multiple-criteria decision-making methods in selecting a seismic upgrading strategy and earthquake engineering.

***doi**: 10.5829/ije.2020.33.08b.06*

NOMENCLATURE

D	seismic design category	S_S	maximum considered earthquake (MCE) spectral acceleration at short periods (g)
I	risk category	S_1	maximum considered earthquake (MCE) spectral acceleration at 1-s period (g)
EDP	Engineering Demand Parameter	Sa	seismic scale factor
x_{ij}	element of the decision matrix	r_{ij}	element of the normalized matrix
E_j	entropy of each criterion	m	number of alternatives
n	number of criteria	w_j	weight of each criterion
$[R]$	normalized decision matrix	d_j	uncertainty of jth criterion
$[V]$	weighted normalized decision matrix	C_j	relative distance to positive ideal alternative
S_i^+, S_i^-	distance from positive and negative ideal alternatives	$A^{(+)}, A^{(-)}$	Positive and negative ideal criterion

1. INTRODUCTION

In recent decades, the dual systems of steel moment-resisting frames and RC shear walls have found extensive application as lateral load-resisting systems for high-rise structures in seismically active areas and regions where buildings are exposed to high winds. This system is commonly used in residential, office, and hospital buildings. The underlying reason behind using a steel moment-resisting frame instead of a concrete moment-resisting frame is higher steel strength, smaller cross-section, and easy implementation. Moreover, the

*Corresponding Author Institutional Email: *tehranizadeh@aut.ac.ir* (M. Tehranizadeh)

Please cite this article as: M. S. Barkhordari, M. Tehranizadeh, Ranking Passive Seismic Control Systems by Their Effectiveness in Reducing Responses of High-Rise Buildings with Concrete Shear Walls Using Multiple-Criteria Decision Making, International Journal of Engineering (IJE), IJE TRANSACTIONS B: Applications Vol. 33, No. 8, (August 2020) 1479-1490

concrete curing process in reinforced concrete moment-resisting frames can affect its quality. On the other hand, the concrete shear wall is coupled with the steel moment-resisting frame to enhance structural resistance to lateral loads exerted by wind, earthquake, or the reduction of cross-section area. Structures equipped with this system typically perform well against collapse [1]. Nevertheless, they might suffer from severe damages from significant lateral loads exerted by an earthquake or the wind, which can cause substantial economic losses in turn. An example would be the impacts of the Christchurch Earthquake on structures with this system [2]. This earthquake caused considerable damage to several buildings with the shear wall-frame dual lateral resisting system. Since the repair of the concrete shear wall is complicated and may impair the structural performance, it was decided to demolish several shear wall-reinforced structures, inflicting economic and social burdens to many urban areas.

Seismic energy-dissipation mechanisms are commonly considered in design techniques. For example, considering specific places for plastic hinges (at the base of the shear wall and two ends of the beam) allows these points to enter the nonlinear area and energy dissipation in them. An alternative method for energy dissipation is the use of energy dissipation devices. Each device has a specific dissipation mechanism. Madsen et al. [3] investigated the effect of using dampers in different areas of coupling shear walls and found that the placement of dampers between two walls and near the connective beam results in the improvement of responses. Faridani and Capsoni [4] investigated the effects of using viscous damping on coupled shear walls with flexural and shear mechanisms. Analysis results showed that the bending and shear damping mechanisms performed better than the linear classical damping. Ahmed [5] used fluid viscous dampers in reinforced-concrete core wall buildings and showed the reduction of deformation, rotation, and energy demands. Hejazi et al. [6] analyzed structures with concrete shear walls under seismic loading using a 3D model. They sought an optimal place for viscous dampers and found that its placement over the shear wall frame resulted in maximum reduction of placement and element loading. Muscat [7] carried out similar studies. Aydin et al. published a paper in which they investigated the optimum design of viscous dampers in multistorey buildings [8]. Cetin et al. [9] carried out similar studies. The TMD is another type of damper used and investigated by researchers to control the responses of concrete moment-resisting frames [10–13]. For example, Hessabi et al. [14] have examined the application of the tuned mass dampers for improving the performance of base-isolated structures. Chung et al. [15] proposed a new friction damper to control the responses of the RC shear wall system. They showed that the performance of the new friction damper was higher than the coupled wall with a rigid beam. Ahn et al. [16], Bagheri and Oh [17] also conducted similar studies. Base isolators are another structure control strategy. Osgooei et al. [18] used rectangular fiber-reinforced elastomeric isolators to control the responses of a structure with a concrete shear wall and showed that the maximum response is considerably reduced in a structure with an isolator. There are similar studies into the effect of isolators on the response of structures with concrete shear walls [19, 20]. Another critical topic is concrete shear wall modeling. Previous studies relied on certain models for macro modeling of concrete shear walls that were incapable of taking into account the interaction between axial/flexural and shear behavior. Experimental studies have shown the effect of shear deformation even in the responses of slender walls [21–24]. Ignoring the interactions between axial, flexural, and shear loads results in an underestimation of flexural compressive strains and overestimation of lateral load-resisting capacity and shear load demand in the plastic hinge area [25–27]. In addition to the importance of controlling failure and collapse in concrete shear walls, it is essential to reduce the damages of shear wall components. Therefore, there is no clear solution to the problem of selecting the (more efficient) energy dissipation systems between dampers and isolators. As a result, this paper intends to investigate and rank dampers and isolators' effectiveness in controlling and reducing damages in concrete shear walls. On the other hand, such factors as diverse selection criteria and effective parameters (e.g., effect of frequency content of ground motions) make the decision-making problematic to the extent that the existing criteria no longer facilitate the selection or ranking of optimal alternatives and the use of more straightforward methods. As a result, the most common weighting method (entropy weigh method) and multiple attribute decision making method (MCDM) (TOPSIS-Technique for Order Preference by Similarity to Ideal Solution) are employed [28–30].

2. BUILDING SPECIFICATIONS

Five buildings (10, 15, 20, 25, and 30-story) were examined in this paper. The employed systems for these buildings are concrete shear wall-steel frame dual lateral resisting system. Figure 1 shows the typical plan and elevation of the buildings. The building plan consisted of five bays having a width of 4m. The typical height of each story is 4m. The design dead and live loads are, respectively, 5.5 and $2KN/m^2$. The compressive strength of concrete used in wall is assumed to be $40MPa$. The longitudinal rebars with a yield stress of $470MPa$ and the transverse rebars as well as stirrups with a yield stress of $430MPa$ are used as reinforcement. The nominal yield strength of the steel (the steel beams

and columns of the frame) is assumed to be $350MPa$. The dimensional details of the beams, columns, and rebar sections of the concrete shear wall are presented in Appendix A. Damping induced by the structural components (concrete shear wall, beams, and columns) are considered to be 2% and applied using the Rayleigh damping. The gravity framing is considered using the leaning column which is linked to the main structure (Figure 2). Rigid truss elements are used to link the shear wall-steel frame and leaning columns and transfer the P-Delta effect. Table 1 characterizes the building site and design parameters. The design was conducted based on ACI 318 and ASCE 7 [31, 32]. The building was designed based on the modal response spectrum analysis [32]. The first 15 modes were used in the design.

Four different systems were designed and used (viscous damper, friction damper, tuned mass damper, and lead-rubber isolation bearing) for controlling structural response [33]. A similar target damping was considered for all systems-dampers and LRB isolators. In other words, isolators and dampers were designed to provide a 15% damping. Tables 2-5 present the passive seismic control systems specifications. The modal periods of the buildings are shown in Table 6. The viscous damper is modeled with a Two Node Link Element using OpenSees [34, 35]. This element follows a viscous damper hysteretic response [36]. To simulate the friction damper in OpenSees an equivalent uniaxial material composed of different materials that are already available in the OpenSees library with a Two Node Link Element are used [37]. The LRB isolator is modeled with a ZeroLength Element and a uniaxial KikuchiAikenLRB material object. This material model produces nonlinear hysteretic curves of lead-rubber bearings [38]. To simulate the nonlinear response of the reinforced concrete shear walls, a nonlinear Timoshenko element and a nDMaterial MCFT material are utilized [24]. Tuned mass damper is modeled with a ZeroLength Element and Viscous and Elastic materials [39]. Columns and beams are modeled using DispBeamColumn elements, Steel02 material, and Concrete02 material [34, 35].

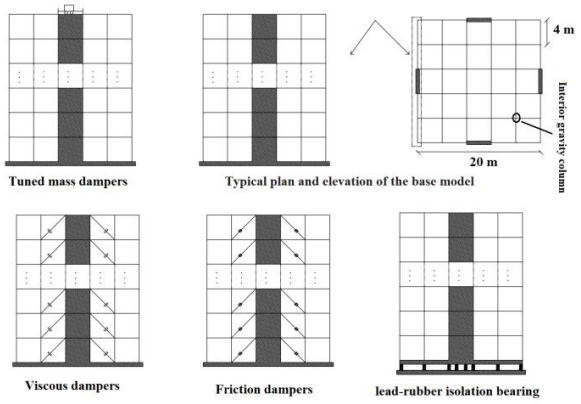

Figure 1. Typical plan and elevation of buildings

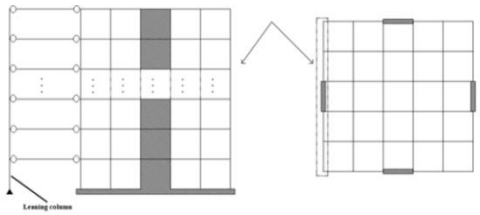

Figure 2. Modeling gravity framing using the leaning column

TABLE 1. Strouhal number for different geometric cases

Latitude	Longitude	Seismic design Cat.	Risk Cat.	Soil classification	S_S (g)	S_1 (g)
35.653 $\circ N$	-120.440 $\circ W$	D	I	D	1.5	0.6

TABLE 2. Viscosity coefficient of nonlinear viscous dampers

Story	10	15	20	25	30
$C\frac{KN\cdot sec^{0.5}}{m^{0.5}}$	400	597	611	810	992

TABLE 3. Slip-load of friction dampers

Story	10	15	20	25	30
Yield strength (slip load) KN	240	170	130	141	150

TABLE 4. Tuned mass dampers

Story	10	15	20	25	30
Mass (ton)	30	45	60	75	90
Stiffness (KN/m)	384	342.5	217.5	248.1	206
C_d $(N.sec/m)$	22550	26050	26784	28728	28512

TABLE 5. Lead-rubber isolation bearing

Story	10	15	20	25	30
Area of rubber (m^2)	0.385	0.442	0.570	0.7	1.227
Thickness of rubber (m)	0.5	0.65	0.8	0.95	1.15
Area of lead plug (m^2)	0.0201	0.024	0.038	0.038	0.057
Yield stress of lead plug $(N/m^2)\times 10^6$	8.82				
Shear modulus of rubber $(N/m^2)\times 10^4$	64				

TABLE 6. Modal periods of the prototype buildings

	Modal periods (sec)				
Story	**10**	**15**	**20**	**25**	**30**
Fixed based	1.61	2.66	3.17	3.8	4.3
Friction	0.98	1.59	1.86	2.08	2.63
LRB	1.81	2.98	3.39	3.89	4.38
TMD	1.79	2.98	3.41	4.06	4.6
Viscous	1.63	2.81	3.22	3.82	4.34

Given that the frequency content of earthquakes differed, which in turn affected the structural responses. This study investigated structures using 50 seismic records. Details of seismic records are presented in Appendix A. Earthquake records with a velocity pulse in the near field are selected from the database of the Pacific Earthquake Engineering Research (PEER) [40]. The minimum magnitude of near-field records is taken as 6.0 and near-field records are within a distance less than 15km to the fault. Given these criteria, total 18 earthquake records (the near field records) are obtained from the PEER database. The first 18 records are the near-field ground motions, and the remaining records are the far-field ground motions. These ground motions were scaled for the maximum considered earthquake (MCE) hazard level. Record scaling in the PEER Ground Motion Database (PGMD, [40]) is accomplished by applying a linear scale factor that does not alter the relative frequency content of the acceleration time series. There are two options for scaling in the PGMD. In this study, the records are scaled to match the target spectrum over a period range (from 0.2T to 1.5T where T is the first mode of vibration). In other words, the average value of the 5% damped response spectra for the suit of motions is not less than ASCE design response spectrum [32]. As an example, responses of the buildings (10, 15, 20, 25, and 30 stories) subjected to the ground motion (No. 1) recorded at the Brawley Airport station during the 1979 Imperial Valley earthquake are illustrated. Figures 3-7 show the responses.

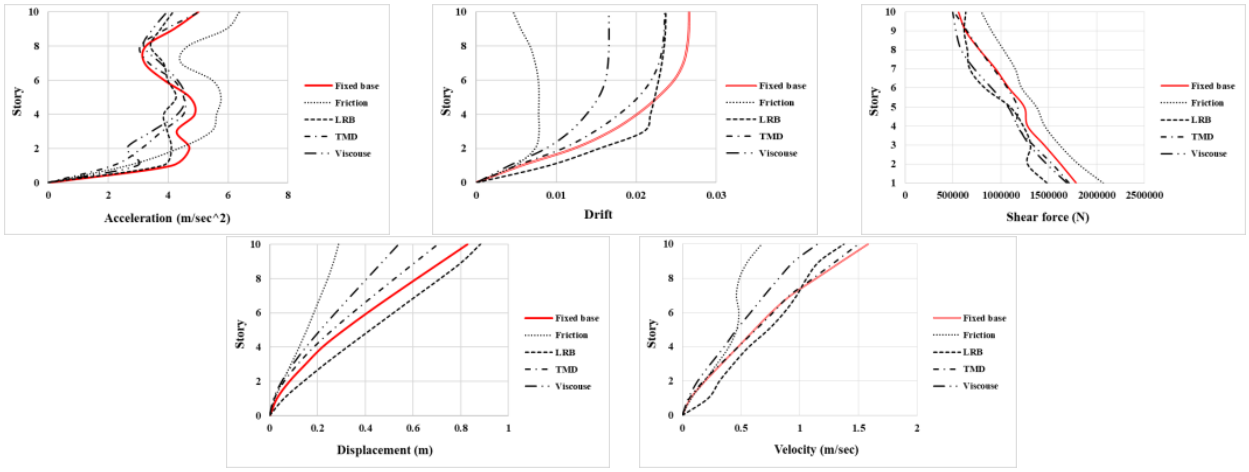

Figure 3. Responses of the 10-story buildings subjected to ground motion No. 1

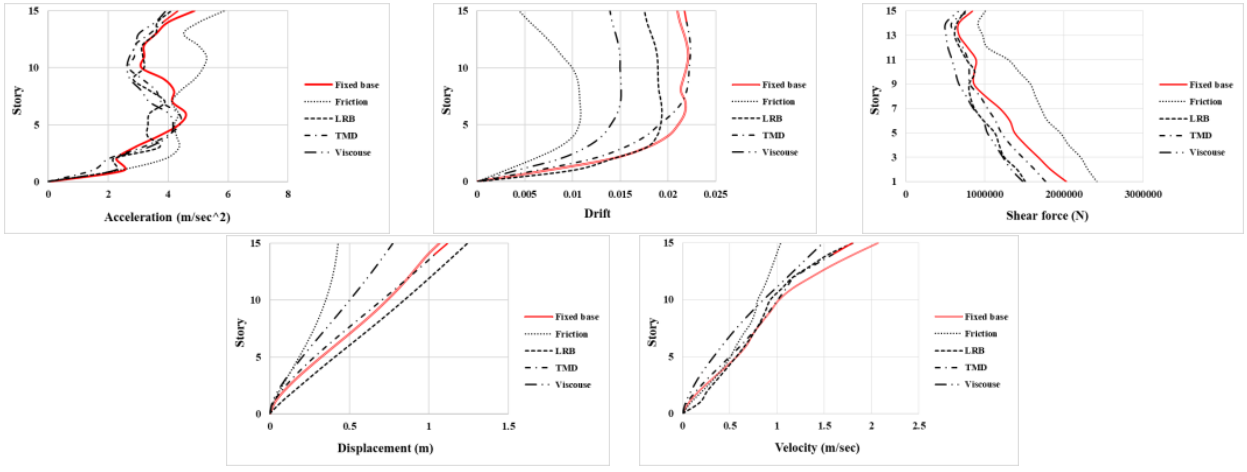

Figure 4. Responses of the 15-story buildings subjected to ground motion No. 1

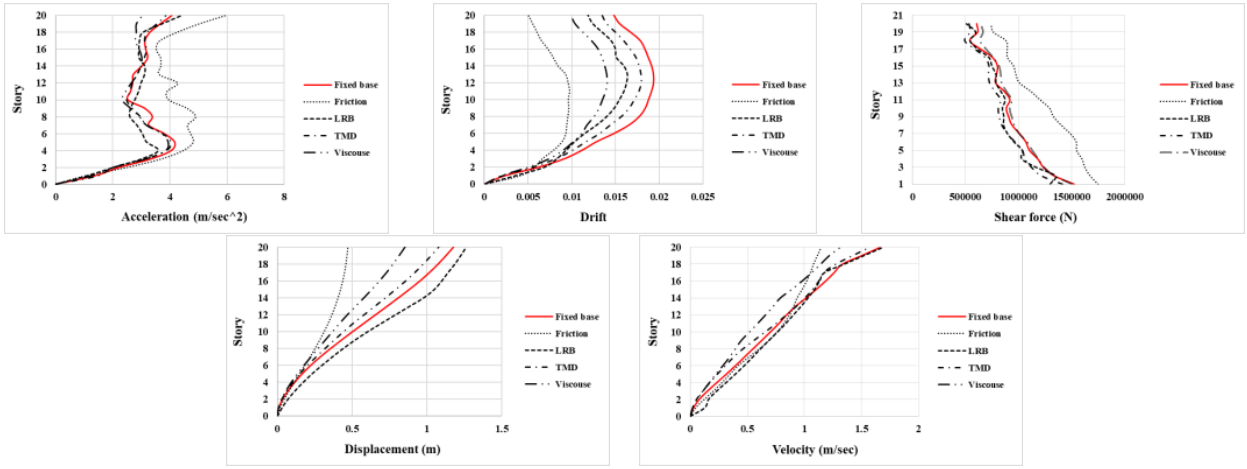

Figure 5. Responses of the 20-story buildings subjected to ground motion No. 1

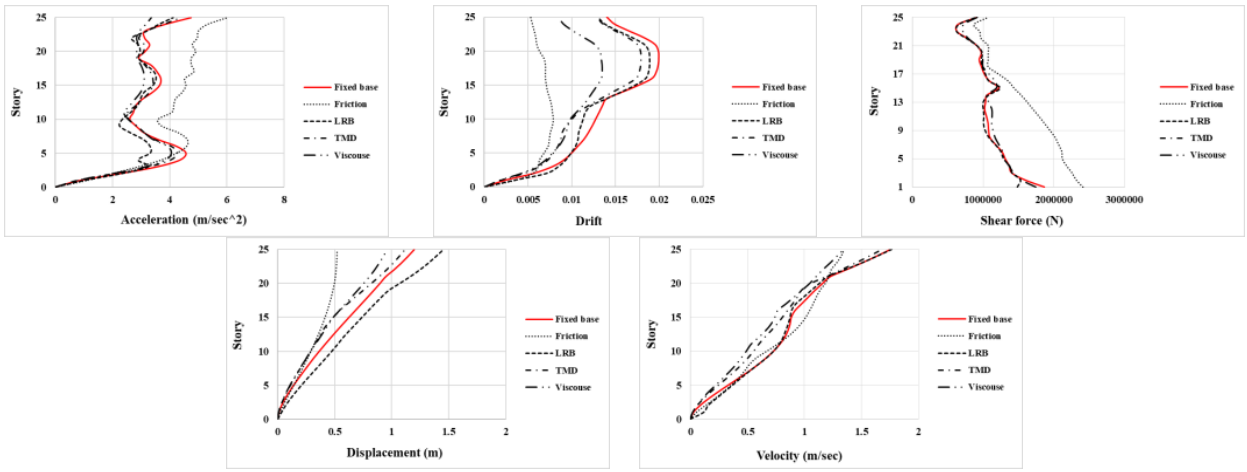

Figure 6. Responses of the 25-story buildings subjected to ground motion No. 1

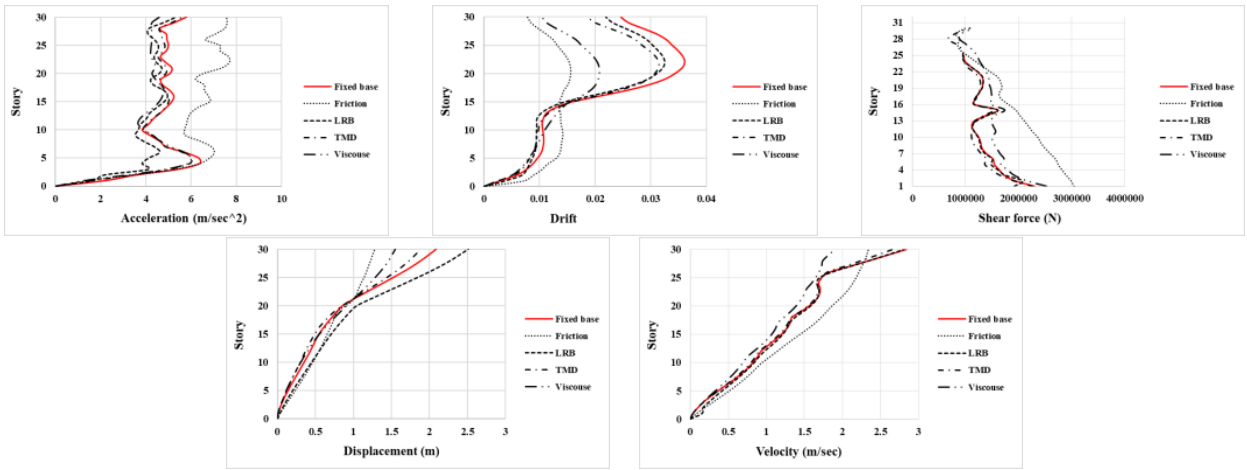

Figure 7. Responses of the 30-story buildings subjected to ground motion No. 1

3. MCDM

In the majority of cases, decision making is convenient when it is based on some measure or criterion. We can use the multiple-criteria decision-making method (MCDM) to deal with definite and explicit criterion. In fact, the MCDM was used to solve a decision making problem by identifying the best alternative that fulfilled a

set number of criteria. The story drift, base shear, the story displacement, story velocity, and story acceleration of different systems can be regarded as criteria to form the decision matrix. One way to calculate these criteria is by using the maximum obtained for each system under the 50 seismic records. However, this approach does not outline the relationship between the ground motion and the given criterion explicitly. For example, a structure subjected to a seismic excitation with the scale factor of 1.2 may have the maximum drift of 1.5%; whereas, its maximum drift under another seismic excitation with the scale factor of 0.5 is 2.1%, which is because the ground motion naturally undergoes random changes and has different frequency contents. For high-rise structures, the effects of the higher modes are also significant. As a result, it was tried to define a measure to consider it via establishing a relationship between the scale factor and criteria (story drift, base shear, story velocity, and acceleration) and used the values of this measure instead of direct use of criteria in the decision matrix.

3. 1. Measure Describing the System Reaction

As was mentioned earlier, the decision matrix should express the relationship between input and output. Regarding section 2 and that earthquakes are scaled using the scale factor, the establishment of a relationship between the scale factor and story drift, story displacement, base shear, story velocity, and story acceleration can contribute to a better understanding of the effect of ground motion frequency content on structural response and its effect on the decision matrix. As a result, the rate of the scale factor against each structural response was adopted as a criterion. The numerical value of each criterion was calculated using Equation (1):

$$Indicator\,Value\,(IV) = \Delta EDP - \Delta Sa$$
$$where:$$
$$\Delta EDP = \left(\frac{EDP_n - EDP_{\min}}{EDP_{\max} - EDP_{\min}}\right) - \left(\frac{EDP_{n-1} - EDP_{\min}}{EDP_{\max} - EDP_{\min}}\right) \quad (1)$$
$$\Delta Sa = \left(\frac{Sa_n - Sa_{\min}}{Sa_{\max} - Sa_{\min}}\right) - \left(\frac{Sa_{n-1} - Sa_{\min}}{Sa_{\max} - Sa_{\min}}\right)$$

In Equation (1), the Engineering Demand Parameter (EDP) is a structural response (e.g., Drift), and Sa represents the seismic scale factor. In Equation (1), the maximum value of structural responses is considered for EDP with different value. For example, there are 15 drift values for a 15-story building, out of which the maximum value is considered for a specific seismic excitement. As a result, the decision matrix has five criteria (story drift, base shear, story velocity, story displacement, and story acceleration), each of which is related to a measure, and their values are calculated using Equation (1). The concept of negative criterion in decision-making suggests the criterion utility (e.g., cost) reduces as it increases in value. Here too, we are dealing with negative criteria since an increase in these criteria is indicative of weak system performance. The first step in the MCDM is forming the decision matrix (Table 7). Table 7 is obtained using the results of simulations and Equation (1). Each row of this matrix indicates the existing alternatives, and each column represents the score of the alternative for each criterion. The second step is the matrix normalization. Normalization is a column-specific operation and distinctively applied to the column specific to each criterion. If each element of the decision matrix is represented by x_{ij}, the element of the normalized matrix will be calculated by Equation (2):

$$r_{ij} = \frac{x_{ij}}{\sum_{i=1}^{m} x_{ij}} \quad (2)$$

In Equation (2), m is the number of alternatives. Table 8 shows the normalized matrix.

TABLE 7. Decision matrix

10 story	**Index value**				
	Accel.	**Disp.**	**Drift**	**Base Shear**	**Vel.**
Friction	7.89	7.68	6.55	7.54	7.02
LRB	7.27	11.8	11.49	7.23	8.97
TMD	8.126	10.765	7.79	7.21	8.27
Viscous	5.79	10.32	9.02	5.21	9.02
15 story	**Index value**				
	Accel.	**Disp.**	**Drift**	**Base Shear**	**Vel.**
Friction	9.712	8.554	7.02	7.066	7.62
LRB	9.435	12.224	8.594	6.648	9.493
TMD	9.921	11.486	8.488	6.709	7.785
Viscous	9.284	8.971	7.893	7.132	7.968
20 story	**Index value**				
	Accel.	**Disp.**	**Drift**	**Base Shear**	**Vel.**
Friction	7.812	5.465	4.839	4.593	5.611
LRB	7.874	10	7.24	5.829	6.823
TMD	7.777	8.675	7.831	6.468	7.308
Viscous	7.834	10.851	9.227	6.385	7.373
25 story	**Index value**				
	Accel.	**Disp.**	**Drift**	**Base Shear**	**Vel.**
Friction	5.983	4.734	4.731	4.734	5.581
LRB	6.786	9.052	6.612	5.422	6.194
TMD	7.08	9.2	7.325	5.07	5.542
Viscous	7.166	9.927	9.147	5.334	6.04
30 story	**Index value**				
	Accel.	**Disp.**	**Drift**	**Base Shear**	**Vel.**
Friction	4.214	5.744	5.114	5.027	5.109
LRB	6.958	11.539	8.123	4.784	4.501
TMD	7.232	13.198	9.095	5.128	5.499
Viscous	7.299	8.929	6.198	4.664	5.152

TABLE 8. The normalized decision matrix

10 story	Index value				
	Accel.	**Disp.**	**Drift**	**Base Shear**	**Vel.**
Friction	0.2713	0.1893	0.1879	0.2773	0.2109
LRB	0.2500	0.2908	0.3297	0.2659	0.2695
TMD	0.2794	0.2653	0.2235	0.2651	0.2485
Viscous	0.1991	0.2544	0.2588	0.1916	0.2710
15 story	**Index value**				
	Accel.	**Disp.**	**Drift**	**Base Shear**	**Vel.**
Friction	0.2532	0.2074	0.2194	0.2564	0.2318
LRB	0.2460	0.2964	0.2686	0.2412	0.2888
TMD	0.2586	0.2785	0.2652	0.2434	0.2368
Viscous	0.2420	0.2175	0.2466	0.2588	0.2424
20 story	**Index value**				
	Accel.	**Disp.**	**Drift**	**Base Shear**	**Vel.**
Friction	0.2496	0.1561	0.1660	0.1973	0.2069
LRB	0.2515	0.2857	0.2484	0.2504	0.2516
TMD	0.2484	0.2479	0.2687	0.2778	0.2695
Viscous	0.2503	0.3101	0.3166	0.2743	0.2719
25 story	**Index value**				
	Accel.	**Disp.**	**Drift**	**Base Shear**	**Vel.**
Friction	0.2214	0.1438	0.1700	0.2302	0.2389
LRB	0.2511	0.2750	0.2377	0.2637	0.2651
TMD	0.2620	0.2795	0.2633	0.2465	0.2372
Viscous	0.2652	0.3016	0.3288	0.2594	0.2585
30 story	**Index value**				
	Accel.	**Disp.**	**Drift**	**Base Shear**	**Vel.**
Friction	0.1639	0.1457	0.1792	0.2564	0.2521
LRB	0.2707	0.2927	0.2847	0.2440	0.2221
TMD	0.2813	0.3348	0.3187	0.2615	0.2714
Viscous	0.2839	0.2265	0.2172	0.2379	0.2542

After the normalization, all criteria are converted into positive criteria using Equation (3):

$$r_{ij}^{+} = 1 - r_{ij} \tag{3}$$

Hereafter, these matrices are used to calculate the weights of criteria.

3. 2. Indicators Weight In this step, the importance of each criterion relative to others is determined by the entropy method. This method uses the elements of the decision matrix to determine the weight of the criteria. Based on this method, the importance of a criterion grows with increasing the dispersion of its value. The weights of criteria are calculated in the following steps:

1. Normalizing the decision matrix with m alternatives and n criteria

2. Calculating the entropy of each criterion using Equation (4):

$$E_j = -\frac{1}{ln(m)} \cdot \left(\sum_{i=1}^{m} r_{ij}^{+} \cdot ln(r_{ij}^{+})\right) \tag{4}$$

3. Determining uncertainty of j[th] criterion using Equation (5):

$$d_j = 1 - E_j \tag{5}$$

4. Determining the weight of each criterion using Equation (6):

$$w_j = \frac{d_j}{\sum_{j=1}^{m} d_j} \tag{6}$$

The weight of each criterion was calculated using the entropy method and presented in Table 9.

3. 3. Decision-Making Model The last decision-making step is selecting a decision-making model to prioritize the criteria. For this purpose, the TOPSIS [41] technique was employed. Based on this technique, the selected criterion should have the minimum distance from the positive ideal solution (the best solution) and the maximum distance from the negative ideal solution (the worst solution). The solution steps are as follows:1) Formation of decision matrix, 2) Normalization of decision matrix and conversion of negative criteria into positive ones$[R]$3) Outlining the measure weight vector, 4) Forming of weighted normalized decision matrix $[V] = \{W\}[R]$, 5) Determining positive and negative ideal alternatives (Equation (7)). The positive ideal criterion is actually a vector of the best alternatives on each column; whereas, the worst alternatives in each column are used as the negative ideal criterion.

$$\begin{aligned} A^{(+)} &= \{Max(V_{i1}) \quad \dots \quad Max(V_{in})\} \\ A^{(-)} &= \{Min(V_{i1}) \quad \dots \quad Min(V_{in})\} \end{aligned} \tag{7}$$

6) Calculation of distance from positive and negative ideal alternatives using using Equation (8):

$$S_i^{+} = \sqrt{\sum_{j=1}^{n}(V_{ij} - A_j^{+})^2}, S_i^{-} = \sqrt{\sum_{j=1}^{n}(V_{ij} - A_j^{-})^2} \tag{8}$$

TABLE 9. Weight of each criterion using Entropy method

Building	Acc.	Disp.	Drift	Base Shear	Velocity
10-story	0.1454	0.2089	0.3833	0.1751	0.0871
15- story	0.0209	0.5868	0.2594	0.0282	0.1044
20-story	0.0014	0.4282	0.3613	0.1262	0.0827
25-story	0.0381	0.5219	0.3987	0.0220	0.0191
30-story	0.2352	0.4651	0.2626	0.0086	0.0283

7) The last step was the calculation of the relative distance to positive ideal alternative using Equation (9):

$$C_j = \frac{S_j^{(-)}}{S_j^{(+)}+S_j^{(-)}} \quad (9)$$

The parameter C_j remains in the 0-1 range. A criterion gets closer to the positive ideal alternative with increasing C_j. The criteria are ranked based on the greater C_j which is taken as the score for each criterion. The score or value of C_j for each criterion is presented in Tables 10.

4. DISCUSSION

According to Tables 10, based on the criteria of choice and conditions, the friction damper ranked first for all buildings (10, 15, 20, 25, and 30 stories). In other words, the use of the friction dampers results in better control over structural behavior under seismic excitement, which can be attributed to the characteristics of this damper. In the nonlinear viscous damper, the damping ratio of the nonlinear viscous damper depends on the vibration frequency (ω) and maximum displacement of the two ends of the damper (u_{max} or modal displacement shape

TABLE 10. Score and rank of each criterion in buildings

	System	Score	Rank
10-story	Friction	0.38838	1
	LRB	0.03746	4
	TMD	0.3057	2
	Viscous	0.26846	3
15-story	Friction	0.4667	1
	LRB	0.0049	4
	TMD	0.1233	3
	Viscous	0.4051	2
20-story	Friction	0.599	1
	LRB	0.1794	3
	TMD	0.2185	2
	Viscous	0.0031	4
25-story	Friction	0.62039	1
	LRB	0.21506	2
	TMD	0.16359	3
	Viscous	0.00096	4
30-story	Friction	0.564	1
	LRB	0.1242	3
	TMD	0.0035	4
	Viscous	0.3081	2

(Equation (10)). As a result, the superiority of the friction damper over the nonlinear viscous damper is due to the former's independence of velocity and vibration frequency [42].

$$F_D = C_{NL} \cdot |u|^{\alpha} \cdot \mathrm{sgn}(u) \quad , \quad \alpha = 0.5 \, , \qquad C_{NL} = C_L \cdot \frac{\pi}{\lambda} \cdot (u_{\max} \cdot \omega)^{1-\alpha} \quad (10)$$

Although the friction damper causes extra structural stiffness, this stiffness is eliminated after damper slip and used to resist small seismic and wind excitements.

Another point is the effect of higher modes on the behavior of structures with concrete shear walls [43]. The second and even the third vibration modes in high-rise structures can increase the shear and flexural force demand. For instance, Yang et al. [44] showed that structural responses increase with increasing the magnitude of an earthquake due to the involvement of higher modes; besides, the deformation of different modes and related internal forces increases after the formation of a plastic hinge at the wall base. This behavior can result in formation of other plastic hinges in the height of the wall. The tuned mass damper is designed based on the first mode frequency. Studies have shown that the TMD sensitivity to frequency changes results in yield reduction. Results showed that the TMD ranked last among other alternatives for 30-story building. As an advantage of such systems (TMDs), they can respond to small levels of excitation. But, the performance of TMD is very sensitive to the natural frequency of structures and damping percentage of the damper. In addition, the effectiveness of a tuned mass damper is constrained by the maximum weight that can be practically placed on top of the structure. One solution is to investigate the use of the multiple mass dampers vertically distributed in the height of the structure in tall buildings based on modal analysis, which is recommended for future studies. A large number of base-isolated high-rise buildings were built (Thousand Tower with a height of 135 m, Sendai MT building with a height of 84.9 m, and super high-rise building in Japan with a height of 177.4 m [45, 46]) in recent decades. In the low-rise and mid-rise buildings, the use of base isolators extends the first period, which in turn reduces the load exerted on the structure. However, the extension of the period is negligible in high-rise buildings. The main reason for using base isolators in high-rise buildings (e.g., Tokyo Skytree East Tower, Taiwan Tan Tzu Medical center, and Japan Thousand Tower and Sendai MT building) is to dissipate large portions of seismic energy. Nevertheless, numerical results indicated that this system failed in obtaining a good score and rank. In addition, recent study suggests that, even for design-level earthquake, base isolation is not effective for near-field earthquakes [47]. Therefore, it did not meet the main goal, i.e., the seismic energy attraction and dissipation, and thus did not adequately

control structural responses relative to other existing alternatives. One solution, that should be examined, is using multiple base isolators vertically distributed in the height of the structure -or another type of isolator, such as friction pendulum isolators in high-rise buildings. Considering the above paragraphs, it can be concluded that it is difficult to determine and select a seismic passive control system without using a multi-criteria decision-making method.

5. CONCLUSION

This study investigated the control and reduction of seismic responses of high-rise buildings with concrete shear walls using viscous dampers, friction dampers, TMD, and lead-rubber isolation bearings. Five buildings with 10, 15, 20, 25, and 30 stories were reinforced with four passive control systems mentioned earlier. Next, the structures were subjected to 50 seismic records. The structural responses (acceleration, drift, velocity, displacement, and base shear) were adopted as criteria, and quantitative indicators were defined to establish a relationship between the inputs (ground motions) and the outputs (responses). At the end, the TOPSIS was found to be the best method of reinforcement and controlling the damage and responses of the concrete shear wall. Based on the criteria of choice and systems conditions, results showed that the friction damper had the highest score, ranking first among the discussed dampers in all buildings, followed by other dampers, with differences based on the number of stories. For example, the TMD ranked second and fourth in 20-story and 30-story buildings, respectively. Therefore, structural characteristics (e.g., periods of the first to third modes) and their relationship with the mode level, selected control system characteristics (e.g., the dependence of viscous damper performance on velocity), and frequency content is among parameters that affect the structural responses. Due to the complexity of the problem, it is recommended to use the multi criterion decision making (MCDM) under these scenarios.

6. REFERENCES

1. Lu, X., Lu, X., Guan, H., and Ye, L. "Collapse simulation of reinforced concrete high-rise building induced by extreme earthquakes." ***Earthquake Engineering and Structural Dynamics***, Vol. 42, No. 5, (2013), 705–723. https://doi.org/10.1002/eqe.2240
2. Xu, Z., Lu, X., Cheng, Q., Guan, H., Deng, L., and Zhang, Z. "A smart phone-based system for post-earthquake investigations of building damage." ***International Journal of Disaster Risk Reduction***, Vol. 27, (2018), 214–222. https://doi.org/10.1016/j.ijdrr.2017.10.008
3. Madsen, L. P. B., Thambiratnam, D. P., and Perera, N. J. "Seismic response of building structures with dampers in shear walls." ***Computers and Structures***, Vol. 81, No. 4, (2003), 239–253. https://doi.org/10.1016/S0045-7949(02)00441-8
4. Moghadasi Faridani, H., and Capsoni, A. "Investigation of the effects of viscous damping mechanisms on structural characteristics in coupled shear walls." ***Engineering Structures***, Vol. 116, (2016), 121–139. https://doi.org/10.1016/j.engstruct.2016.02.031
5. Ahmed, M. "Fluid viscous dampers locations in reinforced-concrete core wall buildings." ***Proceedings of the Institution of Civil Engineers - Structures and Buildings***, Vol. 170, No. 1, (2017), 33–50. https://doi.org/10.1680/jstbu.16.00007
6. Hejazi, F., Ostovar, N., and Bashir, A. "Seismic response of shear wall with viscous damping system." In Lecture Notes in Civil Engineering (Vol. 9, pp. 595–607). Springer. https://doi.org/10.1007/978-981-10-8016-6_46
7. Muscat, O. "Examination of Shear Walls Retrofitted with Fluid Viscous Dampers." ***International Journal of Pure and Applied Mathematics***, Vol. 118, No. 24, (2018), 1–10. Retrieved from https://acadpubl.eu/hub/2018-118-24/4/631.pdf
8. Aydin, E., Öztürk, B., and Dutkiewicz, M. "Analysis of efficiency of passive dampers in multistorey buildings." ***Journal of Sound and Vibration***, Vol. 439, (2019), 17–28. https://doi.org/10.1016/j.jsv.2018.09.031
9. Cetin, H., Aydin, E., and Ozturk, B. "Optimal Design and Distribution of Viscous Dampers for Shear Building Structures Under Seismic Excitations." ***Frontiers in Built Environment***, Vol. 5, No. 90, (2019), 1–13. https://doi.org/10.3389/fbuil.2019.00090
10. Jiang, Q., Lu, X., Guan, H., and Ye, X. "Shaking table model test and FE analysis of a reinforced concrete mega-frame structure with tuned mass dampers." ***The Structural Design of Tall and Special Buildings***, Vol. 23, No. 18, (2014), 1426–1442. https://doi.org/10.1002/tal.1150
11. Mate, N. U., Bakre, S. V., and Jaiswal, O. R. "Seismic Pounding Response of Singled-Degree-of-Freedom Elastic and Inelastic Structures Using Passive Tuned Mass Damper." ***International Journal of Civil Engineering***, Vol. 15, No. 7, (2017), 991–1005. https://doi.org/10.1007/s40999-017-0178-7
12. Kamgar, R., Samea, P., and Khatibinia, M. "Optimizing parameters of tuned mass damper subjected to critical earthquake." ***The Structural Design of Tall and Special Buildings***, Vol. 27, No. 7, (2018), e1460. https://doi.org/10.1002/tal.1460
13. Reza, M. S., Jaafar, K., Shams, S., and Azad, A. K. "Tube shear wall interaction of high rise building and influence of damper on its dynamic behavior." In 7th Brunei International Conference on Engineering and Technology (BICET 2018) (Vol. 2018, pp. 1–4). Institution of Engineering and Technology. https://doi.org/10.1049/cp.2018.1609
14. Hessabi, R. M., Mercan, O., and Ozturk, B. "Exploring the effects of tuned mass dampers on the seismic performance of structures with nonlinear base isolation systems." ***Earthquake and Structures***, Vol. 12, No. 3, (2017), 285–296. https://doi.org/10.12989/eas.2017.12.3.285
15. Chung, H.-S., Moon, B.-W., Lee, S.-K., Park, J.-H., and Min, K.-W. "Seismic performance of friction dampers using flexure of rc shear wall system." ***The Structural Design of Tall and Special Buildings***, Vol. 18, No. 7, (2009), 807–822. https://doi.org/10.1002/tal.524
16. Ahn, T.-S., Kim, Y.-J., and Kim, S.-D. "Large-Scale Testing of Coupled Shear Wall Structures with Damping Devices." ***Advances in Structural Engineering***, Vol. 16, No. 11, (2013), 1943–1955. https://doi.org/10.1260/1369-4332.16.11.1943
17. Bagheri, B., and Oh, S. H. "Seismic Design of Coupled Shear Wall Building Linked by Hysteretic Dampers using Energy Based Seismic Design." ***International Journal of Steel Structures***, Vol.

18, No. 1, (2018), 225–253. https://doi.org/10.1007/s13296-018-0318-1

18. Osgooei, P. M., Tait, M. J., and Konstantinidis, D. "Seismic Isolation of a Shear Wall Structure Using Rectangular Fiber-Reinforced Elastomeric Isolators." ***Journal of Structural Engineering***, Vol. 142, No. 2, (2016), 04015116. https://doi.org/10.1061/(ASCE)ST.1943-541X.0001376
19. Li, A., Yang, C., Xie, L., Liu, L., and Zeng, D. "Research on the Rational Yield Ratio of Isolation System and Its Application to the Design of Seismically Isolated Reinforced Concrete Frame-Core Tube Tall Buildings." ***Applied Sciences***, Vol. 7, No. 11, (2017), 1191–1210. https://doi.org/10.3390/app7111191
20. Wang, W., Li, A., and Wang, X. "Seismic performance of precast concrete shear wall structure with improved assembly horizontal wall connections." ***Bulletin of Earthquake Engineering***, Vol. 16, No. 9, (2018), 4133–4158. https://doi.org/10.1007/s10518-018-0348-2
21. Massone, L., and Wallace, J. "Load-deformation responses of slender reinforced concrete walls." ***Structural Journal***, Vol. 101, No. 1, (2004), 103–113. Retrieved from https://www.concrete.org/publications/internationalconcreteabstractsportal/m/details/id/13003
22. Thomsen, J., and Wallace, J. Displacement based design of reinforced concrete structural walls: an experimental investigation of walls with rectangular and t-shaped cross-sections: a dissertation, Doctoral dissertation, Clarkson University, Potsdam, United States (1995).
23. Tran, T. A., and Wallace, J. W. "Cyclic Testing of Moderate-Aspect-Ratio Reinforced Concrete Structural Walls." ***ACI Structural Journal***, Vol. 112, No. 6, (2015), 653–665. Retrieved from 110.14359/51687907
24. Barkhordari, M. S., Tehranizadeh, M., and Scott, M. H. "Numerical modeling strategy for predicting the response of RC walls using Timoshenko theory." ***Magazine of Concrete Research***, (2020), 1–70. https://doi.org/10.1680/jmacr.19.00542
25. Kolozvari, K., Orakcal, K., and Wallace, J. W. "Modeling of Cyclic Shear-Flexure Interaction in Reinforced Concrete Structural Walls. I: Theory." ***Journal of Structural Engineering***, Vol. 141, No. 5, (2015), 04014135. https://doi.org/10.1061/(ASCE)ST.1943-541X.0001059
26. Orakcal, K., and Wallace, J.W., "Flexural Modeling of Reinforced Concrete Walls— Experimental Verification." ***ACI Structural Journal***, Vol. 103, No. 2, (2006), 196–206. https://doi.org/10.1061/(ASCE)0733-9445(2004)130:4(618)
27. Kolozvari, K., and Wallace, J. W. "Practical Nonlinear Modeling of Reinforced Concrete Structural Walls." ***Journal of Structural Engineering***, Vol. 142, No. 12, (2016), G4016001. https://doi.org/10.1061/(ASCE)ST.1943-541X.0001492
28. Formisano, A., Castaldo, C., and Chiumiento, G. "Optimal seismic upgrading of a reinforced concrete school building with metal-based devices using an efficient multi-criteria decision-making method." ***Structure and Infrastructure Engineering***, Vol. 13, No. 11, (2017), 1373–1389. https://doi.org/10.1080/15732479.2016.1268174
29. Invidiata, A., Lavagna, M., and Ghisi, E. "Selecting design strategies using multi-criteria decision making to improve the sustainability of buildings." ***Building and Environment***, Vol. 139, (2018), 58–68. https://doi.org/10.1016/j.buildenv.2018.04.041
30. Mosalam, K. M., Alibrandi, U., Lee, H., and Armengou, J. "Performance-based engineering and multi-criteria decision analysis for sustainable and resilient building design." ***Structural Safety***, Vol. 74, (2018), 1–13. https://doi.org/10.1016/j.strusafe.2018.03.005
31. ACI 318-08, "Building code requirements for structural concrete (ACI 318-08) and commentary", American Concrete Institute, (2014).
32. ASCE Standard, "Minimum design loads for buildings and other structures", American society of civil engineers/structural engineering institute, Reston, Virginia, (2010).
33. Takewaki, I. Building control with passive dampers: optimal performance-based design for earthquakes. John Wiley & Sons, (2011).
34. McKenna, F., Scott, M. H., and Fenves, G. L. "Nonlinear Finite-Element Analysis Software Architecture Using Object Composition." ***Journal of Computing in Civil Engineering***, Vol. 24, No. 1, (2010), 95–107. https://doi.org/10.1061/(ASCE)CP.1943-5487.0000002
35. Mazzoni, S., McKenna, F., Scott, M. H., and Fenves, G. L., "OpenSees command language manual", Pacific Earthquake Engineering Research (PEER) Center, (2007).
36. Akçelyan, S., and Lignos, D. "Dynamic Analyses of 1-Story Moment Frame with Viscous Dampers", (2015).
37. Aiken, I. D., Nims, D. K., Whittaker, A. S., and Kelly, J. M. "Testing of Passive Energy Dissipation Systems." ***Earthquake Spectra***, Vol. 9, No. 3, (1993), 335–370. https://doi.org/10.1193/1.1585720
38. Kikuchi, M., Nakamura, T., and Aiken, I. D. "Three-dimensional analysis for square seismic isolation bearings under large shear deformations and high axial loads." ***Earthquake Engineering & Structural Dynamics***, Vol. 39, No. 13, (2010), 1513–1531. https://doi.org/10.1002/eqe.1042
39. Ramezani, M., Bathaei, A., and Ghorbani-Tanha, A. K. "Application of artificial neural networks in optimal tuning of tuned mass dampers implemented in high-rise buildings subjected to wind load." ***Earthquake Engineering and Engineering Vibration***, Vol. 17, No. 4, (2018), 903–915. https://doi.org/10.1007/s11803-018-0483-4
40. Ancheta, T., Darragh, R., Stewart, J., and Seyhan, E. "PEER 2013/03: PEER NGA-West2 Database." Pacific Earthquake Engineering Research, (3013).
41. Papathanasiou, J., and Ploskas, N. Multiple Criteria Decision Aid (Vol. 136, pp.57-89), Springer International Publishing, (2018). https://doi.org/10.1007/978-3-319-91648-4
42. Hanson, R., and Soong, T. Seismic design with supplemental energy dissipation devices. Earthquake Engineering Research Institute, (2001).
43. Rodriguez, M. E., Restrepo, J. I., and Carr, A. J. "Earthquake-induced floor horizontal accelerations in buildings." ***Earthquake Engineering and Structural Dynamics***, Vol. 31, No. 3, (2002), 693–718. https://doi.org/10.1002/eqe.149
44. Yang, T.Y., and Moehle, J.P., "The Tall Buildings Initiative." In 14th World Conference on Earthquake Engineering (Vol. 12). Airiti Press, Inc., (2008). https://doi.org/10.5297/ser.1201.002
45. Komuro, T., Nishikawa, Y., Kimura, Y., and Isshiki, Y. "Development and Realization of Base Isolation System for High-Rise Buildings." ***Journal of Advanced Concrete Technology***, Vol. 3, No. 2, (2005), 233–239. https://doi.org/10.3151/jact.3.233
46. Wang, S., Du, D., and Liu, W. "Research on key issues about seismic isolation design of high-rise buildings structure." In Proceedings of the 11th World Conference on Seismic Isolation, Energy Dissipation and Active Vibration Control of Structures, (2009), 17–21.
47. Bhandari, M., Bharti, S. D., Shrimali, M. K., and Datta, T. K. "The Numerical Study of Base-Isolated Buildings Under Near-Field and Far-Field Earthquakes." ***Journal of Earthquake Engineering***, Vol. 22, No. 6, (2018), 989–1007. https://doi.org/10.1080/13632469.2016.1269698

7. APPENDIX A

TABLE A.1. Shear wall section of the prototype buildings

Building	No. of story	Thickness (cm)	Longitudinal Rein.	Transverse Rein.
10-story	1-4	35	#6@20cm	$8.8cm^2/m$
	5-8	30	#5@20cm	$7.5cm^2/m$
	9-10	25	#4@20cm	$6.3cm^2/m$
15-story	1-5	30	#5@20cm	$7.5cm^2/m$
	6-10	30	#4@25cm	$6.3cm^2/m$
	11-15	25	#4@25cm	$6.3cm^2/m$
20-story	1-5	35	#6@20cm	$8.8cm^2/m$
	6-10	30	#5@20cm	$7.5cm^2/m$
	11-15	25	#4@20cm	$6.3cm^2/m$
	16-20	25	#4@25cm	$6.3cm^2/m$
25-story	1-5	35	#6@15cm	$8.8cm^2/m$
	6-10	30	#6@20cm	$7.5cm^2/m$
	11-15	30	#5@20cm	$7.5cm^2/m$
	16-20	30	#4@20cm	$7.5cm^2/m$
	21-25	25	#4@25cm	$6.3cm^2/m$
30-story	1-5	35	#7@20cm	$8.8cm^2/m$
	6-10	35	#6@20cm	$8.8cm^2/m$
	11-15	30	#5@20cm	$7.5cm^2/m$
	16-20	30	#5@25cm	$7.5cm^2/m$
	21-25	25	#4@20cm	$6.3cm^2/m$
	26-30	25	#4@25cm	$6.3cm^2/m$

TABLE A.2. Characteristics of the selected records

No.	Earthquake Name	Station	year	Mag.
1	"Imperial Valley-06"	"Brawley Airport"	1979	6.53
2	"Imperial Valley-06"	"El Centro Array #10"	1979	6.53
3	"Loma Prieta"	"Gilroy - Historic Bldg."	1989	6.93
4	"Loma Prieta"	"Gilroy Array #2"	1989	6.93
5	"Loma Prieta"	"Gilroy Array #3"	1989	6.93
6	"Loma Prieta"	"Saratoga - W Valley."	1989	6.93
7	"Chi-Chi_ Taiwan"	"CHY101"	1999	7.62
8	"Duzce_ Turkey"	"Bolu"	1999	7.14
9	"Chuetsu-oki_ Japan"	"Joetsu Kakizakiku "	2007	6.8
10	"Dar. _ New Zealand"	"Riccarton High School "	2010	7
11	"El Mayor _ Mexico"	"El Centro Array #12"	2010	7.2
12	"El Mayor _ Mexico"	"Westside Elementary "	2010	7.2
13	"Imperial Valley-06"	"El Centro Array #11"	1979	6.53
14	"Superstition Hills-02"	"Poe Road (temp)"	1987	6.54
15	"Superstition Hills-02"	"Westmorland Fire Sta"	1987	6.54
16	"Northridge-01"	"Beverly Hills - 14145"	1994	6.69
17	"Kobe_ Japan"	"Amagasaki"	1995	6.9
18	"Kocaeli_ Turkey"	"Duzce"	1999	7.51
19	"Iwate_ Japan"	"MYG005"	2008	6.9
20	"El Mayor _ Mexico"	"CERRO PRIETO "	2010	7.2
21	"El Mayor _ Mexico"	"MICHOACAN DE "	2010	7.2
22	"El Mayor _ Mexico"	"RIITO"	2010	7.2
23	"El Mayor _ Mexico"	"EJIDO SALTILLO"	2010	7.2
24	"Dar. _ New Zealand"	"DFHS"	2010	7
25	"Chri. _ New Zealand"	"Papanui High School "	2011	6.2
26	"Northern Calif-03"	"Ferndale City Hall"	1954	6.5
27	"Coalinga-01"	"Parkfield - Fault Zone 14"	1983	6.36
28	"Loma Prieta"	"Hollister - South & Pine"	1989	6.93
29	"Loma Prieta"	"Hollister City Hall"	1989	6.93
30	"Kobe_ Japan"	"Sakai"	1995	6.9
31	"Kobe_ Japan"	"Yae"	1995	6.9
32	"Chi-Chi_ Taiwan"	"TCU038"	1999	7.62
33	"Chi-Chi_ Taiwan"	"TCU112"	1999	7.62
34	"Chi-Chi_ Taiwan"	"TCU117"	1999	7.62
35	"Chi-Chi_ Taiwan"	"TCU118"	1999	7.62
36	"St Elias_ Alaska"	"Icy Bay"	1979	7.54
37	"Chi-Chi_ Taiwan-03"	"CHY025"	1999	6.2
38	"Chi-Chi_ Taiwan-03"	"TCU065"	1999	6.2
39	"Chuetsu-oki_ Japan"	"Joetsu City"	2007	6.8
40	"Iwate_ Japan"	"Nakashinden Town"	2008	6.9
41	"Iwate_ Japan"	"Semine Kurihara City"	2008	6.9
42	"Iwate_ Japan"	"Yokote Masuda Tamati Masu"	2008	6.9
43	"El Mayor _ Mexico"	"TAMAULIPAS"	2010	7.2
44	"El Mayor _ Mexico"	"El Centro - Meloland "	2010	7.2
45	"El Mayor _ Mexico"	"El Centro - Geotechnic"	2010	7.2

Persian Abstract

چکیده

در این مقاله توانایی میراگر جرمی تنظیم‌شونده، میراگر ویسکوز، میراگر اصطکاکی و جداگر هسته سربی در کاهش خرابی و پاسخ‌های سازه‌های بلند دارای دیوار برشی بتنی مورد بررسی قرار گرفته است. پنج ساختمان با تعداد طبقات۱۵،۱۰، ۲۰،۲۵ و ۳۰ طبقه به همراه سیستم‌های کنترل لرزه‌ای غیرفعال تحت اثر ۵۰ رکورد زلزله با استفاده از نرم‌افزار OpenSees تحلیل شده‌اند. پاسخ‌های سازه (شتاب، دریفت، جابه‌جایی، سرعت و برش پایه) به عنوان معیار در نظر گرفته شده است. برای ایجاد ارتباط بین ورودی (زلزله) و خروجی (پاسخ‌های سازه) با تعریف کردن یک شاخص، مقدار کمی بی‌بعد برای هر معیار محاسبه شده است. در نهایت با استفاده از روش تصمیم‌گیری چند معیاره، گزینه‌های موجود برای مقاوم‌سازی و کنترل پاسخ سازه‌ها رتبه‌بندی شده اند.